THOROUGH EVALUATION OF BRIDGE COLUMNS AFFECTED BY ALKALI-SILICA REACTION (ASR)

Leandro Sanchez[1], Benoit Fournier[2], Josée Bastien[2], Denis Mitchell[3], Martin Noel[1]

[1]University of Ottawa, Ottawa, ON, CANADA

[2]Université Laval, Québec, QC, CANADA

[3]McGill University, Montréal, QC, CANADA

Abstract

Robert-Bourassa/Charest viaduct (Quebec, Canada) was a bridge structure severely affected by alkali-silica reaction (ASR). Over the years, several inspection surveys and analyses confirmed that the coarse aggregate used in the construction (local siliceous limestone) was alkali-reactive and for many years monitoring and laboratory tests were carried out on the different elements of the structure. In 2010-2011, the viaduct was demolished, which gave the opportunity of obtaining two 3-meter sections of the reinforced columns, one coming from an exposed site and the other from a non-exposed one (i.e. under the bridge deck). This paper presents the results of the mechanical evaluation as well as the appraisal of the stress-state of the stirrups of both concrete columns. Results show that damage varies according to the columns exposure conditions and coring direction. Concerns may arise regarding the potential for stirrups yielding in the field.

Keywords: Alkali-aggregate reaction; structural implications; aging infrastructure; concrete structures.

1 INTRODUCTION

Robert-Bourassa/Charest (RBC) viaduct was a highway bridge structure (Quebec, Canada) that was built in 1966 using an alkali-silica reactive limestone aggregate (dark-grey, fine-grained Ordovician limestone). The bridge was made of a deck resting on reinforced concrete Y-shaped columns, themselves supported by massive concrete foundations (Figure 1a). No specific information is available on the concrete mix designs used for construction; however, technical reports indicate that the 28-day concrete design strengths were 24 MPa for the foundation blocks and 28 MPa for the columns and decks [1].

Over the last 3 decades, many signs of distress developed on the various elements of the structure. This included extensive steel corrosion and concrete delamination/spalling at the level of the deck; map cracking, scaling, disaggregation and pop-outs affecting the massive concrete foundations due to ASR and freeze-thaw (FT) cycles; as well as concrete spalling and steel corrosion on the columns and foundations exposed to de-icing salt-water sprayed from traffic on the Robert-Bourassa highway [2]. Numerous site inspection surveys, expansion monitoring and laboratory tests were performed on the RBC structure and cores extracted from its different structural elements. From the above investigations, Bérubé et al, 2005 developed a guide for the diagnosis, prognosis and management of AAR-affected structures using a number of laboratory tests (such as the Stiffness Damage Test (SDT), Damage Rating Index (DRI), residual expansion, water soluble alkali, etc.) to assess the degree of deterioration of a concrete element as well as its potential for further damage [3]. Although quite promising, some test method procedures proposed in this guide, were more-or-less diagnostic and, thus, limited the usefulness of the acquired data.

Prior and during the demolition of the RBC bridge in 2010/2011, two 3-meter sections of the reinforced columns (one coming from an exposed site and the other from a non-exposed one) were sawed (Figure 1b) and stored in the laboratory at Université Laval (Quebec, Canada) (Figure 1c and d). Then, several cores were drilled along the three main directions (Longitudinal, Vertical and Traversal) from each of them. Therefore the condition assessment of the columns was performed as proposed by [4-8]. Moreover, at designated locations, the concrete cover of the columns was removed for assessing the stress-state of the stirrups, since earlier studies in Japan showed the potential of rupture of stirrups in concrete structural elements affected by ASR [9].

* Correspondence to: Leandro.sanchez@uottawa.ca

2 SCOPE OF THE WORK

This paper presents the test results of the condition assessment performed on the cores extracted from two 3-m sections of reinforced columns recovered during RBC demolition. Moreover, the analysis of the stress-state of the stirrups was carried out. The objectives of this work are to test the reliability of the multi-level approach proposed by [4-8] for the condition assessment of aging infrastructure, and to discuss the potential structural implications of ASR in affected concrete structures.

3 MATERIAL PROPERTIES

Two 3-meter sections of RBC reinforced columns (one coming from an exposed site (E) and the other from a non-exposed one (i.e. under the bridge deck - NE)) were sawed (Figure 1B) and stored in the laboratory. It is important to mention that due to the severity of its deterioration, the E column has been wrapped with FRP sheets back in 2000 (Figure 1D). Several cores were drilled along the three main directions (Longitudinal, Vertical and Traversal) from each of the above columns and mechanical testing (i.e. SDT, modulus of elasticity and compressive strength) performed on those cores. Moreover, at specific locations, the concrete cover of the columns was removed and the stress-state of the columns stirrups was analysed. The following sections present the description of the test procedures used for this work.

3.1 Mechanical Testing

Compressive strength test

Compressive strength was determined according to ASTM C 39 on four cores from each of the E and NE columns. The results obtained from the non-exposed column (NE) were used to establish the maximum load for stiffness damage testing (i.e. 40% of this value, as by [4-6]). The compressive strengths of the four cores extracted from the exposed column (E) were analysed for comparing the strength reductions caused by ASR in both columns. Description of the compression tests are found in Table 1.

Stiffness Damage Test (SDT)

The *Stiffness Damage Test* (SDT) is currently used to quantify the damage degree of concrete affected by ASR [4-7]. The method is based on cyclic loading (using 40% of the compressive strength of "sound" concrete of similar characteristics/mix design) of concrete samples (cylinders or cores). The full procedure is described in Sanchez et al. [4-6] and the same parameters were adopted in this study. Using a controlled loading rate of 0.10 MPa/s, five cycles of loading/unloading were applied on each set of samples presented in Table 1. Each set is comprised of four to six concrete cores extracted from the same column section and direction (i.e. E vs. NE; Longitudinal, Transverse, and Vertical).

3.2 Stress-state of the stirrups

Besides the above mechanical assessments, evaluations were also performed on the stress-state of the stirrups of both columns (NE & E). Therefore, at designated locations, the concrete cover was removed and the concrete surfaces underneath the stirrups were prepared (Figure 2a). Then, strain gauges were glued on the stirrups in order to measure stress relief after cutting (Figure 2b). Six stirrups were selected for testing at each column, as illustrated in Table 1.

4 RESULTS

4.1 Compressive strength test

The compressive strength results for all the concrete cores tested are illustrated in Figure 3. They ranged from 38.5 to 40.8 MPa for the NE column (average of 40.5 MPa), and from 33.1 to 39.9 (average of 37 MPa) for the E column. As expected, a lower average strength but a higher variability of the test results were obtained from cores extracted from the E column.

4.2 Stiffness Damage Test (SDT)

Figure 4 presents the average results of two SDT output parameters, as described by [4-8]: the *Stiffness Damage Index* (SDI), a measure of the dissipated energy caused by the closure of cracks under compression loading, and the *Plastic Deformation Index* (PDI), which quantifies the slipping across surfaces while the internal cracks close under compression loading. Both indices are a function of the extent of inner cracking present in a given material [4-8]. Table 2 presents all the data obtained in this research (i.e. NE vs E columns; Longitudinal vs. Transverse vs. Vertical cores).

The average SDI values for the NE column ranged from 0.19 to 0.20, whereas from 0.18 to 0.24 for the E column. The average PDI values ranged from 0.12 to 0.15 in the NE column and from 0.13 to 0.18 in E column. Moreover, higher results were obtained in the transverse direction in both columns (direction of less reinforcement, Figure 5).

Figure 6 illustrates the modulus of elasticity values obtained in the analyses of both columns. These correspond to the average values measured from the 2nd and 3rd cycles of stiffness damage testing [4-8]. The average values from NE column varied from 20.5 to 21.9 GPa, whereas they ranged from 18.6 to 22.1 GPa for the E column. E column showed greater damage and thus lower modulus of elasticity compared to the NE, as expected. Moreover, higher variability of the elastic modulus results was found for E column.

4.3 Stirrups cutting

Figure 7 illustrates the stress-relief (μstrains) following the cutting of instrumented stirrups from both columns. It is important to mention that the columns were stored in the laboratory for several weeks before testing (i.e. no more live loads applied to the structural members); so, it is fair to consider that the deformations resulting from stress-relief from the stirrups are entirely (or at least largely) related to ASR expansion.

The stirrups cutting analyses were performed in two ways. First, after cover removal, stirrups were cut at their edges (Figure 5 - location E, due to logistics reasons). However, since the stirrups are normally bent at the edges, sometimes attached and close to the columns ends, analyses were also performed in the middle of the column's cross section (Figure 5 – location M) in order to verify whether higher (and more reliable !) values could be obtained.

E column stirrups presented greater deformation values compared to NE stirrups (as expected), especially when the analyses were performed at the middle of the cross section (Figure 5, location M). Actually, comparing data from the edge cuttings (blue bars) and cuttings in the middle of the cross section (black bars), higher values were found at location M for E column whereas almost similar values were found for NE stirrups. This suggests that better results / more reliable are obtained from cutting in the middle section of the stirrups. The average values obtained after cutting in the middle stirrup sections of the non-exposed and exposed columns were respectively 1290 and 570 μstrain.

5 DISCUSSION

5.1 Condition assessment of RBC columns

Sanchez et al. [4-8] proposed a multi-level approach for the condition assessment of concrete affected by AAR (i.e. ASR and ACR) that is based on a set of microscopic (i.e. *Damage Rating Index* - DRI) and mechanical tests (i.e. *Stiffness Damage Test* – SDT, modulus of elasticity, compressive and tensile strength tests) carried out on cores extracted from the structure investigated. Moreover, the approach aimed at estimating the expansion attained by a given concrete, thus providing important information about the diagnosis, prognosis and possible structural implications of the ASR-affected structure/structural member.

In this regard, Sanchez [4] proposed an overall damage assessment chart highlighting the relationship between the expansion development and the mechanical properties reductions and the progress of microscopic features of deterioration in ASR-affected concrete specimens. In this work, the mechanical step of the overall procedure proposed by [4,8] was applied, and the SDI and PDI parameters were determined for each of the columns.

It is clear from the testing data that the concrete condition (or the indices) changes as a function of the direction of coring. Indeed, in the case of the NE column, cracking seemed somewhat homogeneously oriented/distributed since similar average SDI values (0.19-0.20) were obtained from cores extracted in the three directions. Similar average SDI values were also obtained from cores extracted in the longitudinal and vertical directions in the E columns (0.18-0.19), while cores extracted transversally suggested a higher degree of damage (average SDI of 0.24). This is very likely linked to the asymmetric geometric shape and reinforcement detailing of the columns in the field, which likely influenced the stress-state and consequently the direction and development of the cracks in the E column undergoing higher ASR expansion because of more intense exposure to moisture. Such a phenomenon was actually reported by [10] where heterogeneous 3D restraint in structural members may enhance expansion in the direction of least restraint.

The RBC overpass was built in 1966 using a dark-grey, alkali-silica reactive fine-grained Ordovician limestone [11, 12]. Moreover, technical reports state that the concrete of the foundation blocks was designed to reach 24 MPa at 28 days, while the columns and decks were made of 28 MPa

concrete [1]. Sanchez [4] evaluated the loss in mechanical properties of 25, 35 and 45 MPa concrete mixtures incorporating the same reactive coarse aggregate used in RBC construction, as a function of ASR (unrestrained) expansion. Table 3 presents the results for the 35 MPa mixtures (35 MPa mixtures were selected for comparison since the compressive strength values obtained in NE column were near this value). The results in Table 3 suggest that the expansion attained by the columns would be:

- Based on SDI: 0.12% for NE column; 0.20% for E column;
- Based on PDI: 0.05% for NE column; 0.12% for E column;

Indeed, the above should be considered in a very broad way, since RBC mixtures do not necessarily present the same characteristics from those used in [4]. Moreover, the studies performed by [4] were developed in concrete samples undergoing free expansion in the laboratory, which is quite different from the 3-D stress-state present in the field. Despite these well-known differences, the estimated expansion attained by RBC columns through the use of SDT output parameters still gives an idea of the damage degree in both columns, representing very likely a more conservative scenario (worse) than the real field condition, which is interesting for safety reasons.

5.2. Structural implications of ASR

Theoretically, it is well established that the strength and stiffness of reinforced concrete columns can be greatly influenced by changes in the mechanical properties of affected concrete. The elasticity modulus, and in some cases the compressive strength of the concrete can be reduced due to internal cracking resulting from AAR expansion and damage. Lower stiffness of the concrete will result in more stress carried by the compression reinforcement, which may lead to yielding. As a result of delamination of the concrete cover, buckling of the longitudinal reinforcement is also possible if the spacing of the transverse ties is too large, and external confinement may be necessary to prevent brittle failure. Finally, the restrained expansion will increase the compressive stress in the concrete and may lead to premature concrete crushing before the steel yields in compression, although this is not likely to occur in practice [13]. On the other hand, the post-cracking stiffness and yield strength under axial compression loading can also increase as a result of the initial AAR-induced tensile strain in the reinforcement coupled with the volumetric expansion of the concrete which engages the longitudinal and transverse reinforcement leading to better confinement of the core concrete [14]. Therefore, the actual response of structural columns affect by AAR is highly dependent on the level of expansion, reinforcement ratio, and level of confinement provided by transverse ties.

Regarding the data of both compressive strength and modulus of elasticity determinations for both columns, one verifies that, as stated in the literature, compressive strength is not really a concern for the AAR affected concrete [4]. As observed in the case of concretes undergoing unrestrained ASR expansion, cracking at low and moderate expansion levels (up to about 0.10-0.12%) is mainly found in the reactive particles with limited extension into the cement paste, thus inducing limited reductions in compressive strengths. Thus, as stated in [1], concretes of RBC columns should likely have a 28-day strength ≥28 MPa, which was confirmed from core testing (Figure 3). First of all, this means that the concrete used for the columns probably presented strength greater than 28 MPa at 28 days. However, the E column seems to have lower values of compressive strength compared to NE column, yet they are still greater than their 28-day values.

Fairly low elastic modulus values were obtained for the E column, indicating the presence of microcracking due to AAR, especially within the aggregate particles, as by [4, 7]. However, it should be noted that unrestrained uniaxial values of modulus of elasticity cannot be directly applied in the condition assessment of AAR affected structural members due to 3-D stress-states always found in the field. Therefore, these results can just be treated as indicators of inner cracking caused by AAR, similarly to the SDI and PDI indices.

Beyond that, one of the critical issues in ASR-affected structural members is the progressive swelling that may cause yielding and rupture of the reinforcement bars [9]. In this work, the multi-level approach proposed by Sanchez and discussed in the previous section was used to estimate the expansion attained by both NE and E columns, with values between 0.05%-0.12% for NE column and between 0.12%-0.20% for E column. In addition to the above material's testing, six stirrups were selected and cut from each column, in order to understand their stress-state. Results showed that E column presented higher (and almost double) values than NE column (1290 and 570 μstrains, respectively), agreeing with the results from material's testing, especially in the transversal direction. The results obtained for E column seem fairly high, especially because the columns were stored in the laboratory before testing and thus no live loads were still acting on the members when the stirrups were cut. Therefore, those values might be directly linked to AAR and highlight a potential concern

for stirrups yielding of the AAR affected element investigated.

5.3. Remaining tests methods

In this work, the multi-level approach proposed by [4] could not be entirely performed due to time and space constraints. However, as showed in [4,8] the coupling of microscopic data with mechanical behaviour of affected concrete is what actually becomes the approach so interesting. Therefore, to complete the testing campaign, the Damage Rating Index will be performed in 3 cores (200 cm^2 each) from the three directions of both columns. It is strongly believed that these final and thinner analyses will elucidate and further explain the data obtained through the mechanical procedures. Finally, microscopic examination of companion core samples is in progress and is expected to bring additional information regarding the extent and potential preferential orientation of cracking within the structural members investigated.

6 CONCLUSIONS

After carrying out the multi-level approach proposed by [4-8] on cores extracted from non-exposed and exposed (i.e. more ASR-affected) RBC columns, as well as evaluating the potential yielding of reinforcement (stirrups) in the above elements, one can conclude that:

- Different damage degrees are measured according to the coring direction and environmental conditions (i.e. exposed vs non-exposed; longitudinal, vertical and transversal);
- Cores extracted from the exposed column showed more damage than the non-exposed ones, especially those extracted in the transverse direction which is the direction of least restraint in the above columns;
- The compressive strength of the AAR affected concrete does not seem to be a problem, at least for the low to moderate stage of the chemical reaction identified in the specimens.
- Concerns may arise regarding yielding of the stirrups in those columns exposed to ASR-inducing conditions (e.g. external columns exposed to moisture), especially considering that the solicitation on those columns might be greater whether the structure was still in service (e.g. live loads, load from the bridge deck) which could increase the values found;
- The damage chart proposed by [4], through the use of SDI and PDI parameters (i.e. the greater the parameters, the greater the overall ASR damage) is intended and was used in this work to provide an estimate of the AAR-expansion reached to date, information critical for the management and structural appraisal of ASR-affected aging infrastructures. Moreover, according to the results, it likely provides a conservative scenario compared to real structural members in service, since it was developed on ASR-affected specimens undergoing free expansion under accelerated curing conditions in the laboratory.

7 REFERENCES

[1] ICAAR Visit Report. 2000. Report of the visit of structures affected by AAR in the Quebec City area. 11th International conference on alkali-aggregate reaction, Quebec, Canada

[2] Bérubé, MA, Smaoui, N, Fournier, B, Bissonnette, B, Durand, B. (2005a): Evaluation of the expansion attained to date by concrete affected by ASR - Part III: Application to existing structures. Canadian Journal of Civil Engineering, 32, 463-479.

[3] Bérubé, MA, Smaoui, N, Bissonnette, B, Fournier, B. (2005b) : Outil d'évaluation et de gestion des ouvrages d'art affectés de réactions alcalis-silice (RAS). Studies and research on Transports, Minister of Quebec Transportation, September, 140 p.

[4] Sanchez, LFM. (2014): Contribution to the assessment of damage in aging concrete infrastructures affected by alkali-aggregate reaction, PhD thesis, Department of Geology and Geological Engineering, Université Laval, Québec, Canada.

[5] Sanchez, LFM, Fournier, B, Jolin M, Bastien, J. (2014) : Evaluation of the Stiffness Damage Test (SDT) as a tool for assessing damage in concrete due to ASR: test loading and output responses for concretes incorporating fine or coarse reactive aggregates. Cement and Concrete Research, 56, 213-229.

[6] Sanchez, LFM, Fournier, B, Jolin M, Bastien, J. (2015a) : Evaluation of the Stiffness Damage Test (SDT) as a tool for assessing damage in concrete due to ASR: input parameters and variability of the test responses. Construction and Building Materials, 77, 20-32.

[7] Sanchez, LFM, Fournier, B, Jolin M, Duchesne, J. (2015b) : Reliable quantification of AAR damage through assessment of the damage rating index (DRI). Cement and Concrete Research, 67, 74-92.

[8] Sanchez, LFM, Fournier, B, Jolin M, Bastien, J, Mitchell, D. (2015c) : Overall damage assessment of concrete distressed due to alkali-silica reaction and freezing and thawing cycles using microscopic and mechanical tools. Construction Materials Conference (CONMAT), August, Whistler, Canada

[9] Inoue, S, Mikata, Y, Takahashi, Y, Inamasu, K. (2012) : Residual shear capacity of ASR damaged reinforced concrete beams with ruptured stirrups. 14th International conference on alkali-aggregate reaction (ICAAR). Texas, USA.

[10] Multon, S, Toulemonde, F. (2010) : Effect of moisture conditions and transfers on alkali silica reaction damaged structures. Cement and Concrete Research, 40, 924–934.

[11] Fournier, B, Bérubé, MA. (1991) : Évaluation du potentiel de réactivité alcaline des granulats à béton produits dans les Basses-Terres du Saint-Laurent du Québec (Canada). Revue canadienne de génie civil, 18(2), 282-296.

[12] Sanchez, L, Salva, P, Fournier, B, Jolin, M, Pouliot, N, Hovington, A. (2012) : Evaluation of damage in the concrete elements of the overpass "Du Vallon Charest" after nearly 60 years in service. Proc 14th Int. Conf. on AAR, May 20-25th 2012, Austin (Texas), electronic.

[13] Multon, S, Dubroca, S, Seignol, J-F, Toutlemonde, F. (2004): Flexural Strength of Beams Affected by ASR. 12th ICAAR, Beijing, China.

[14] Pleau, R., Bérubé, M. Pigeon, M., Fournier, B., Raphael, S. (1989): Mechanical behavior of concrete affected by ASR. 8th ICAAR, Kyoto, Japan.

TABLE 1: Testing matrix.

Mix design tested	Tests methods	Column type[1]					
		Exposed			Non-exposed		
		L	V	T	L	V	T
25, 35 and 45MPa	Compressive strength	2	-	2	2	-	2
	Stiffness Damage Test/Modulus of elasticity	6	6	6	6	6	6
	Stirrups cutting	-	-	6	-	-	6
Total number of concrete cores – 44 Total number of stirrups analysed – 12							

[1] Cores extracted in the longitudinal (L), vertical (V) and Transverse (T) directions.

TABLE 2: SDT results of the cores drilled from the exposed and non-exposed columns section at three different directions.

Specimen	Condition	Direction	SDI	PDI	E (GPa)	SDI $_{avg}$	PDI $_{avg}$	E $_{avg}$
2A	Exposed	L	0.21	0.16	17.9	0.19	0.15	19.7
2B	Exposed	L	0.16	0.13	21.5			
3A	Exposed	L	0.18	0.13	16.5	0.18	0.13	18.7
3B	Exposed	L	0.18	0.13	20.8			
4A	Exposed	L	0.18	0.13	18.0	0.18	0.13	18.5
4B	Exposed	L	0.18	0.12	18.9			
					Average values	**0.18**	**0.13**	**18.9**
3A	Exposed	T	0.25	0.21	16.0	0.24	0.19	17.8
3B	Exposed	T	0.22	0.16	19.5			
8A	Exposed	T	0.22	0.16	19.5	0.24	0.19	19.0
8B	Exposed	T	0.26	0.21	18.4			
10A	Exposed	T	0.24	0.18	17.4	0.23	0.17	19.2
10B	Exposed	T	0.22	0.16	20.9			
					Average values	**0.24**	**0.18**	**18.6**
5A	Exposed	V	0.18	0.13	22.5	0.18	0.13	22.9
5B	Exposed	V	0.18	0.13	23.3			
6A	Exposed	V	0.19	0.13	21.2	0.19	0.13	21.4
6B	Exposed	V	0.18	0.13	21.5			
					Average values	**0.18**	**0.13**	**22.1**
1A	Non-exp.	L	0.17	0.11	21.3	0.17	0.11	21.8
1B	Non-exp.	L	0.16	0.10	22.2			
2A	Non-exp.	L	0.22	0.13	19.7	0.20	0.14	21.2
2B	Non-exp.	L	0.17	0.14	22.7			
3A	Non-exp.	L	0.20	0.17	18.4	0.20	0.17	18.4
3B	Non-exp.	L	0.20	0.17	18.4			
					Average values	**0.19**	**0.14**	**20.5**
1A	Non-exp.	T	0.20	0.15	18.8	0.20	0.16	20.0
1B	Non-exp.	T	0.19	0.16	21.2			
5A	Non-exp.	T	0.19	0.14	18.8	0.19	0.14	20.0
5B	Non-exp.	T	0.19	0.14	21.1			
9A	Non-exp.	T	0.20	0.16	17.9	0.20	0.17	19.0
9B	Non-exp.	T	0.20	0.17	20.0			
					Average values	**0.20**	**0.15**	**19.6**
1A	Non-exp.	V	0.18	0.13	24.0	0.18	0.12	23.9
1B	Non-exp.	V	0.18	0.11	23.7			
4A	Non-exp.	V	0.21	0.13	18.7	0.20	0.12	20.0
4B	Non-exp.	V	0.18	0.11	21.2			
					Average values	**0.19**	**0.12**	**21.9**

TABLE 3: SDT results of the cores drilled from the exposed and non-exposed columns section at three different directions [4].

Mixture	Condition	Expansion	SDI	PDI	E (GPa)
35 MPa concrete mixture	Free expansion	0.00%	0.08	0.05	37.5
		0.05%	0.12	0.13	35.1
		0.12%	0.19	0.22	24.8
		0.20%	0.24	0.25	21.9

A - Robert Bourassa/Charest overpass

B - Sawing and preparation of the columns

C- Non-exposed column

D- Exposed column

FIGURE 1: RBC pictures: A) overall structure; B) Sawing and preparation of the columns; C) Non-exposed column and; D) Exposed column.

A – Removal of concrete cover

B – Use of strain gauges to measure stress relief

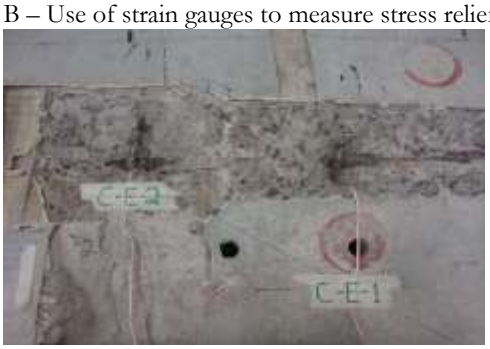

FIGURE 2: RBC columns pictures: A) concrete cover removal and preparation of the surface underneath the stirrups; B) Stirrups with strain gauges glued for measurements of stress-relief white cutting.

A – Non-exposed column

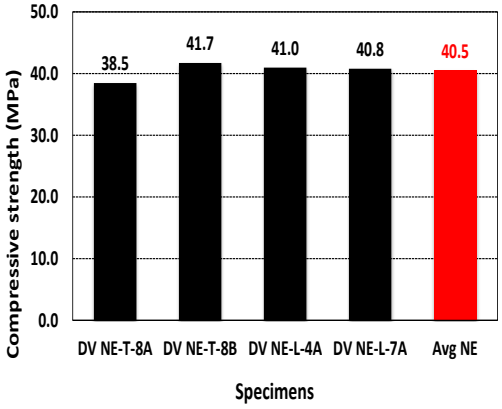

B – Exposed column

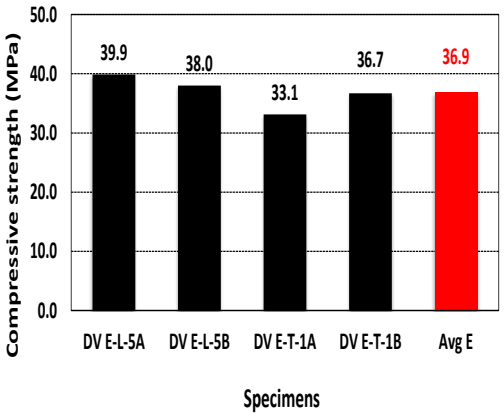

FIGURE 3: Compressive strength values measured on the two columns: a) Non exposed column; B) Exposed column.

A – Non-exposed column

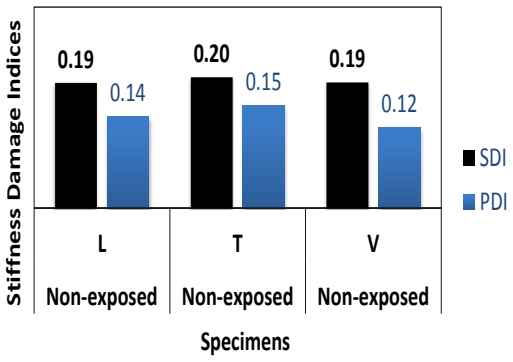

B – Exposed column

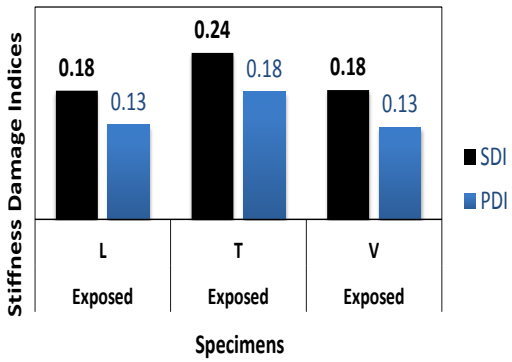

FIGURE 4: SDT indices measured in both non-exposed and exposed columns.

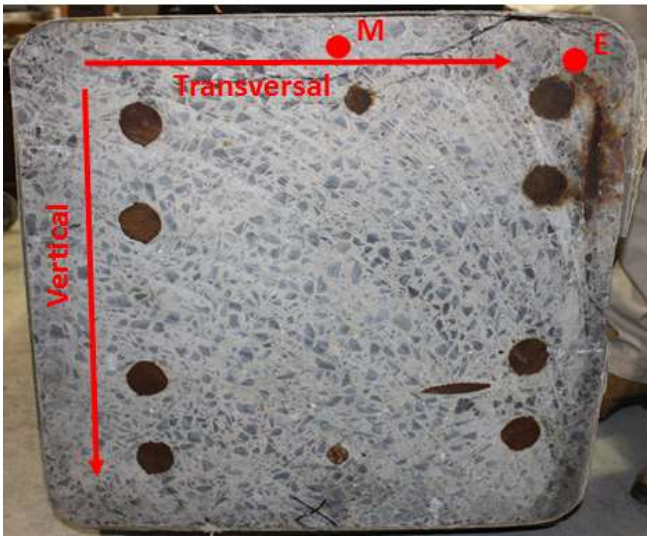

FIGURE 5: CROSS SECTION OF RBC COLUMNS

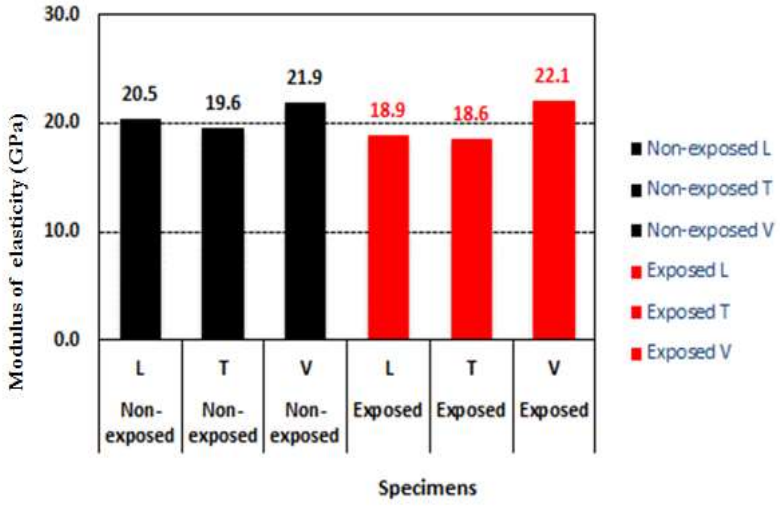

FIGURE 6: Secant modulus of elasticity values measured on the two columns: a) Non-exposed column; B) Exposed column.

A – Non-exposed column

B – Exposed column

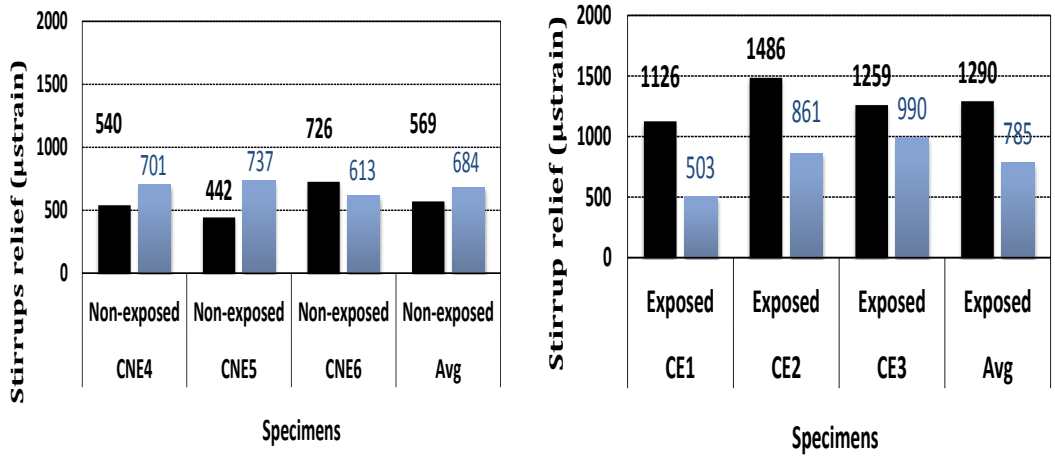

FIGURE 7: Stress-relief measured on the two columns after stirrups cutting: a) Non exposed column; B) Exposed column. Blue bars represent cuts at the stirrups edges (Figure 5 - Location E) and black bars at the middle of the cross section (Figure 5 – location M).